Forced convection heat transfer in micro heat sinks with square and circular configuration

N. Y. Godi[1, 2], L. B. Zhengwuvi[2], M. O. Petinrin[3]

[1]Department of Mechanical Engineering, University of Cape Town, Private Bag X3, Rondebosch, 7701, South Africa

[2]Department of Mechanical Engineering, Modibbo Adama University, P. M. B. 2076, Yola, Adamawa State, Nigeria.

[3]Department of Mechanical Engineering, University of Ibadan, Ibadan, Nigeria

ABSTRACT: This paper reports the results of three-dimensional numerical optimisation of microchannel heat exchanger with square and circular cooling channels. The objective of the optimisation is to maximise the global thermal conductance or minimise global thermal resistance. Response surface optimisation methodology (RSM) is used in the numerical optimisation. A high-density heat flux ($2.5 \times 10^6 W/m^2$) is imposed at the bottom surface of the unit cell microchannel and numerical simulation carried out using ANSYS Fluent commercial software package. The elemental volume and axial length $N = 10\ mm$ of the microchannel were all fixed, while the width was free to morph. The cooling technique employs single-phase water which flows through the rectangular block microchannel heat sink to remove the heat at the bottom of the microchannels in a forced convection laminar flow regime. The velocity of the fluid pumped across the microchannel axial length is the range $400 \leq Re_w \leq 500$. Finite volume method (FVM) is used to descretised the computational domain and computational fluid dynamic (CFD) code employed to solve a series of governing equations. The effect of channel hydraulic diameter and Reynolds number of water-flow on peak wall temperature and minimised temperature are investigated and reported. The numerical results show that the microchannel with square cooling channel has the highest maximised global thermal conductance than the micro heat sink with circular configuration. The result of the numerical study agrees with what is in the open literature.

KEYWORDS: Square configuration, circular configuration, micro heat sink, numerical optimisation, thermal conductance

[Received Aug. 1, 2022; Revised Oct. 8, 2022; Accepted Nov 6, 2022] Print ISSN: 0189-9546 | Online ISSN: 2437-2110

I. INTRODUCTION

The development of thermal devices with high-performance heat transfer rate has been necessitated by the growing energy consumption in the contemporary world. Microchannel heat sinks have drawn a lot of interest on the account of their high capacity for heat dissipation for the thermal management of microelectronics (Gupta *et al*., 2021; Qiu *et al*., 2021; Hajialibabaei and Saghir, 2022). The interest for their outstanding thermal performance has been attributed to high heat transfer surface to volume ratio and compact design, which requires small installation area (He *et al*., 2021). The design principles of a microchannel heat sinks or heat exchangers are based on the heat transfer and pressure drop associated with the device (Han *et al.*, 2012). In the construction of most microchannel heat exchangers, each channel is defined by two parallel plates separated by fins or spacers (Kern & Kraus, 1972). The majority of research on microchannel heat exchangers by researchers concentrated on how structural forms affected performance (Chen *et al*., 2021).

Numerical analysis is widely used to investigate the cooling and optimisation of microchannel heat sinks by several researchers. Gawali and Kamble (2011) numerically studied a rectangular microchannel using forced convection heat transfer with a range of hydraulic diameters, fin spacing and microchannel heights. They used copper as the solid substrate, and the results showed that the most favourable dimension of the flow channel depends on the velocity of the fluid used. Patel and Modi (2012) cooled electronic chips in a silicon single rectangular micro heat sink using CFD code. They concluded water provided better thermal management of electronics than an air-cooling technique. Le *et al*. (2022) used the response surface methodology (RSM) to investigate and optimise the hydraulic and thermal behaviours of multi-nozzle micro-channel heat sinks subjected to dimensional changes in geometry. The predicted values of the pressure drop and Nusselt number of the optimised geometry compared well with such obtained from purely numerical computation. Khan et al. (2022) performed a numerical analysis on the flow and heat transfer characteristics of the perforated pin fin microchannel heat sink in the Reynolds number ranges of 150 to 350. They introduced six evenly spaced cylindrical pin fins with non-dimensionalised perforations of diameters: 0.33, 0.5, 0.67, and 0.83. They discovered improvement of the Nusselt number at the smallest perforation, which is = 0.33, but a declination as the perforation diameter increases, however the highest value

*Corresponding author: nahumgodi@yahoo.co.uk

doi: http://dx.doi.org/10.4314/njtd.v18i4.1272

of overall thermal performance was found to be at perforation size of 0.5.

Chen *et al*. (2021) compared experimentally an optimised structure of microchannel heat exchangers with other three having contrast array of elements under the same constraints under heat transfer efficiency and minimum flow resistance. They were able to establish through experiment that the microchannel heat exchanger with optimised structure demonstrated higher heat transfer efficiency to flow resistance than the three other structures considered. Kose *et al*. (2022) performed parametric CFD and Pareto frontal analyses to establish correlations between the Nusselt number and pumping power of three heat sinks of different microchannel cross-sections with rectangular, triangular and trapezoidal shapes but of the same hydraulic diameter. They found the rectangular microchannel as the configuration with the best thermal-hydraulic performance.

The geometric optimisation technique involving outlining limitations in studying forced convection cooling in microchannel and heat sinks is becoming widespread in understanding thermal management. The idea is based on unknown or missing geometry, which involves stating global objective(s) and restriction(s) of the flow system (Bejan and Lorente, 2011; Olakoyejo *et al.* 2012). The constructal law was firstly introduced by Bejan (2000), which successfully explained the shapes and structures of several physical systems. Constructal law is employed in a range of domains, for example, finding the general ranking of universities around the world, accessing information on the global flow of knowledge (Bejan, 2007, 2009), providing vital information and optimal results in tactical operation and military warfare (Weinerth, 2010), as well as predicting optimal paths to achieve speed for men and women in swimming and athletics competitions (Reis *et al.*, 2004; Bejan and Marden, 2006; Charles and Bejan, 2009; Bejan *et al.*, 2010). Moreover, constructal design has been successfully utilized in the geometric design of microchannels (Y. Li et al., 2014).

Li et al. (2014) employed the constructal law to perform numerical study on water-cooled microchannel heat sinks of four Y-shaped bifurcations at angles 60°, 90°, 120°, and 180° in-between the two arms of the Y-shaped profile. Their study revealed better thermal performance to flow resistance of the Y-shaped bifurcations with 60°and 90° than other configurations. Based on constructal law. Xie *et al*. (2014) numerically studied five different cases of multistage bifurcated microchannels and a case without bifurcation. It was recorded that the heat sinks with multistage bifurcations showed improved overall thermal performance. Qiu *et al*. (2021) also explored the characteristic nature of cobweb to investigate the flow boiling heat transfer performance of two biomimetic microchannels having horizontal and inclined inlets against a conventional-shaped microchannel heat sink. The cobweb-shaped microchannel with horizontal inlet showed enhanced thermal performance and had better stability in flow boiling behavior.

Several studies have been conducted in the field to optimise microchannels with various configurations based on constructal law. Lawal *et al*. (2022) carried out a numerical investigation of effect of constructal design on the performance of a combined heat sink with trapezoidal, inverse trapezoidal, and hexagonal microchannel configurations. Their study revealed that the hexagonal combined and the trapezoidal combined microchannel heat sinks recorded lowest maximum temperature and lowest temperature elevation, respectively. Sun *et al*. (2022) performed a constructal design of a rectangular heat generating body with channel of semi-circular sidewall ribs. The weighted sum function of the multi-objective optimisation determined from the heat transfer and flow performances was enhanced by 8.5%. In Li *et al*. (2021), the aspect ratio of a microchannel heat sink with porous medium at a bottom-wall heat flux of 100 W/cm2 was optimised to minimise the dimensionless entropy generation rate. Their findings revealed that the optimised aspect ratio had a 33.1% reduction in dimensionless entropy generation rate as compared to the initial value. Olakoyejo *et al*. (2012) used both the analytical and numerical methods for constructal design optimisation of cooling channels of square configuration, under laminar forced convection, in a vascularized body subjected to wall heat flux at 10 W/cm3. They obtained the optimal channel geometry with the lowest thermal resistance using the gradient-based optimisation algorithm by minimising the peak temperature in the solid body.

Based on the reviews from previous studies, it can be concluded that geometrical dimensions of flow channels contribute a lot to the overall thermal performance ratio microchannel heat sinks are beneficial to enhance the heat transfer performance. However, the novelty in the present study is in the deployment of the constructal design technique and the ability of the present study to dissipate a large, fixed high-density heat flux of up to 250 W/cm2 as against past studies such as in Olakoyejo *et al*. (2012). The micro heat sink in this study is cooled by increasing the velocity of fluid incrementally across the microchannel heat sink until the imposed heat flux is removed from the bottom, while the previous research pressure difference is employed. And to best of the knowledge of the authors, it has not been clearly shown in literature any of such studies on optimisation of the constructal design of heat sinks with square and circular microchannel cross-sections, whereby the peak temperatures of hotspots are minimised. The higher the peak temperature of a heated spot in a microchannel heat sink the lower its global thermal conductance. The paper showed a numerical optimisation of micro heat sinks with square and circular cooling channels are carried out following the constructal law. Two configurations (square and circular) are designed and optimised to discover the best configuration that minimises the peak temperature or maximises the global thermal conductance. The micro heat sinks designed are cooled using water in a conjugate heat transfer. The results obtained are validated with previous solution.

II. PHYSICAL MODELS OF MICROCHANNEL HEAT SINK

The application of constructal method and technique in the geometric optimisation of microchannel heat sinks (square and circular) with fixed total volume is to determine how geometry affect heat transfer (Bejan & Lorente, 2004, 2006a,

2006b, 2011; Bejan & Sciubba, 1992). Microchannel heat sinks with circular and rectangular cooling channels were designed and the unit cell microchannel simulated. The optimisation technique used in the microchannel heat sinks is based on minimising the peak temperature of the conductive aluminium material which leads to increase in thermal conductance of the entire system. All in the ANSYS workbench, the geometry was created with the Design Modeler, thereafter the mesh grid generation, then the channel flow problem resolved with Fluent and the optimization process was carried out using the RSM tool.

A. Description of physical model

The physical geometry is a model of a micro heat sinks of global volume NHM_x and the computational domain micro heat sinks Figures 1 and 2. The unit cell rectangular block microchannel heat sink used in the simulation has an axial length N, height H and width M Figures 1a and 2b. The flow channel diameter is d and the channel-to-channel spacing is assigned t_3, the distance from the bottom of the rectangular microchannel heat sink to the bottom of the flow channel is t_1, while the distance from the top of the flow channel to the top of the microchannel heat sink is assigned t_2.

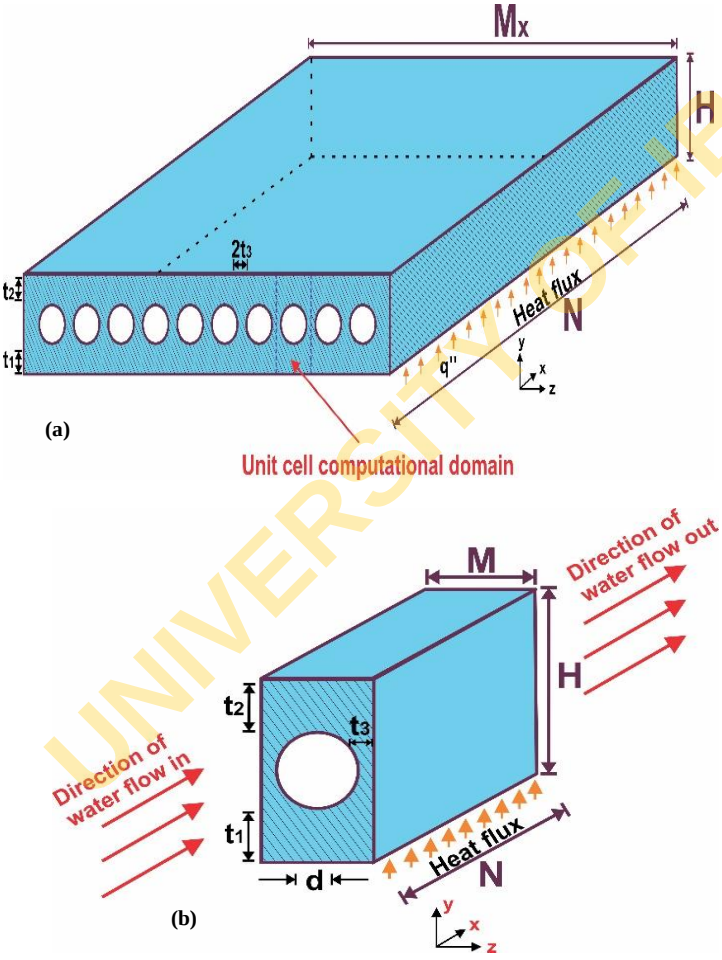

Fig. 1: Diagram of heat sink with (a) circular cooling channel and (b) 3-D diagram unit cell computational domain

The micro heat sink is made from a highly conductive material substrate of aluminium. A heat flux of $q'' = 2.5 \times 10^6 W/m^2$ is applied at the base of the micro heat sink and simulation is carried out on a selected unit cell micro heat sink (Figures 1b and 2b) in accordance with constructal design technique. A forced convection cooling in the heat sink is achieved by allowing cooling fluid (water) to flow through the microchannel entrenched in the solid material.

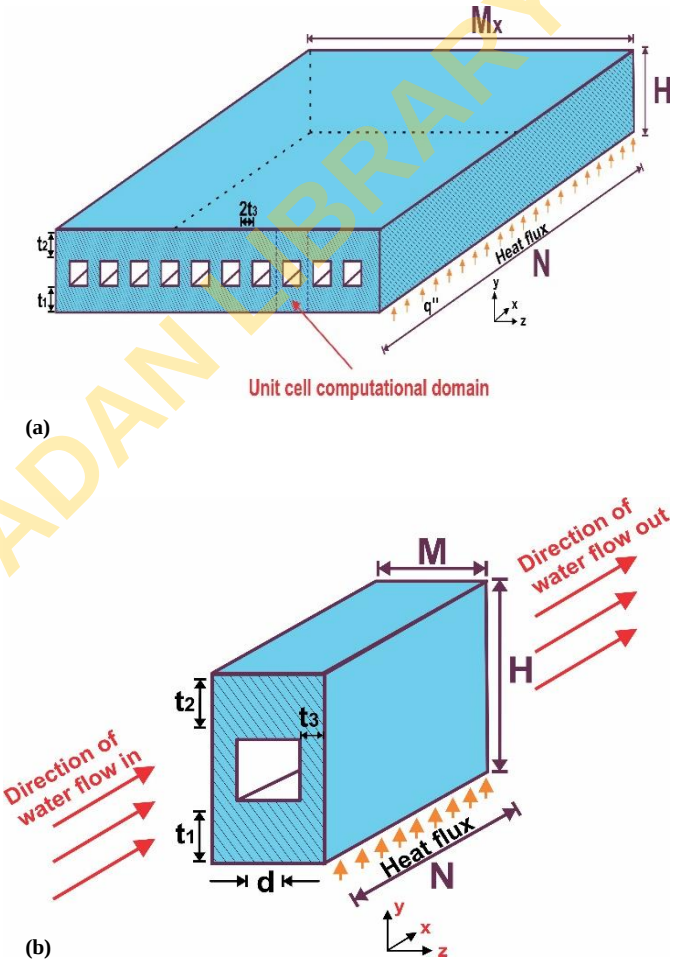

Figure 2: Diagram of heat sink with (a) square cooling channel and (b) 3-D diagram unit cell computational domain

B. Manufacturing constraints, design parameters and optimisation procedure

The axial length N, thickness t_1 and elemental volume v_el (NHM) are fixed, while the width M, t_2, t_3 and d are allowed to vary and are subject to manufacturing limitations. The elemental volume of the microchannel heat sink is shown as follows:

The elemental volume of unit structure with circular and square configurations is

$$v_{el} = MHN = \text{constant} \quad (1)$$

For fixed axial length, the area of the unit structure is

$$A = HM \quad (2)$$

The void fraction ϕ, is given as

$$\phi = \frac{v_c}{v_{el}} \quad (3)$$

The elemental volume flow channel is

$$v_c = \frac{\pi}{4} d^2 N \quad (4)$$

The manufacturing restrictions as defined by deep reactive ion etching (DRIE) procedure used for manufacturing heat sinks (Laermer & Urban, 2003; Madou, 2018) are given as

$$t_1 \geq 50\mu m \quad (5)$$

$$H - (d + t_1) \geq 50\mu m \quad (6)$$

Number of microchannels in the heat sinks arrangement is

$$\mathrm{n} = \frac{HM_x}{HM} = \frac{HM_x}{(2t_3+d)(t_1+t_2+d)} \quad (7)$$

III. GOVERNING EQUATIONS AND BOUNDARY CONDITIONS

The numerical analysis is based on the following assumptions: the system is in a steady state and incompressible flow, water used in the study is in single-phase and laminar flow regime and radiation effects are neglected. Therefore, the governing equations for laminar flow through the microchannel of the heat sink are as follows:

$$\frac{\partial u}{\partial x} + \frac{\partial v}{\partial y} + \frac{\partial w}{\partial z} = 0 \quad (8)$$

$$\rho\left(u\frac{\partial u}{\partial x} + v\frac{\partial u}{\partial y} + w\frac{\partial u}{\partial z}\right) = -\frac{\partial P}{\partial x} + \mu\nabla^2 u \quad (9)$$

$$\rho\left(u\frac{\partial v}{\partial x} + v\frac{\partial v}{\partial y} + w\frac{\partial v}{\partial z}\right) = -\frac{\partial P}{\partial x} + \mu\nabla^2 v \quad (10)$$

$$\rho\left(u\frac{\partial w}{\partial x} + v\frac{\partial w}{\partial y} + w\frac{\partial u}{\partial z}\right) = -\frac{\partial P}{\partial x} + \mu\nabla^2 w \quad (11)$$

$$\rho C_v\left(u\frac{\partial T}{\partial x} + v\frac{\partial T}{\partial y} + w\frac{\partial T}{\partial z}\right) = k\nabla^2 T \quad (12)$$

The momentum equation for the volume occupied by the solid is:

$$\bar{U} = 0 \quad (13)$$

And the energy equation for the solid part of the elemental volume is given as:

$$k_s \nabla^2 T = 0 \quad (14)$$

The continuity of the heat flux at the interface between the solid and the liquid is given as:

$$k_s \frac{\partial T}{\partial n}\Big|_{wall} = k_f \frac{\partial T}{\partial n}\Big|_{wall} \quad (15)$$

The no-slip boundary condition is specified for the fluid at the walls of the channel.

The temperature at the entrance for water is:

$$T = T_{in} \quad (16)$$

And the temperature at the wall outlet is:

$$T = T_{w,L} \quad (17)$$

At the bottom surface of the microchannel heat sink, the thermal conditions imposed are assumed to be:

$$k_s \frac{\partial T}{\partial y} = -q'' \quad (18)$$

The measure of performance or maximised global thermal conductance is given in dimensionless form as (Bello-Ochende *et al*., 2007).

$$C = \frac{q''N}{k_f(T_{max} - T_{in})} \cong \frac{q''N}{k_f(T_{w,N} - T_{in})} \quad (19)$$

where q'' is the heat flux at the heat sink bottom of the microchannel, k_f is the thermal conductivity of the fluid, N is the axial length of computational domain and $\Delta T = T_{w,N} - T_{in}$ is the largest excess temperature attained by the heat sink, which is anticipated to occur at the exit plane of the microchannel.

The C is a function of the optimised design variables and maximum minimum temperature (Olakoyejo *et al*., 2012).

$$C = f\left((d_h)_{opt}, \left(\frac{H}{M}\right)_{opt}, \phi, (T_{max})_{min}\right) \quad (20)$$

The global thermal conductance C is an expression for the ratio of total heat transfer rate divided by the largest excess temperature at any point in the heat sink. The reciprocal of C is the dimensionless global thermal resistance.

A. *Numerical analysis*

The mass, momentum, and energy Eqns. in (8) - (12) were descretised over the computational domain, and numerically solved using the finite volume method by the ANSYS Fluent CFD code (Ighalo, 2010; Laermer & Urban, 2003). This domain was divided into a large number of control volumes, generating the discretised equations containing the conservation principle. The pressure-velocity coupling was executed by the SIMPLE algorithm (Chen and Cheng, 2009; Ismail *et al*., 2009; Chai *et al*., 2011). The second order upwind technique is used to compute the momentum and energy equations. The convergence was established when the normalised residuals (Fig. 3) for the continuity and momentum equations were below 10^{-5} and the energy residuals smaller than 10^{-9}.

1) *Response surface optimisation (RSO)*

The numerical simulation began by constructing the geometry to be optimised using the workbench in design modeler of ANSYS Fluent 18.1 commercial package. The model is meshed, and simulation performed on the computational unit cell. The optimization process starts by deploying the design exploration tool. Once the design parameters to be optimised are assigned, design points (DP) are generated, and design of experiments (DOE) aimed at gathering a representative set of data to compute a response surface and execute optimization for a response surface is obtained. The response surface is thoroughly explained (Khuri and Mukhopadhyay, 2010; Myers *et al*., 2016), and the multi-objectives generic algorithm (MOGA) optimization tool is then employed to find the designed candidates from the response surfaces. The tool provides space to set the optimisation objective, constraint and builds a surrogate model that searches for maximum and minimum values of peak temperature corresponding to optimal design values.

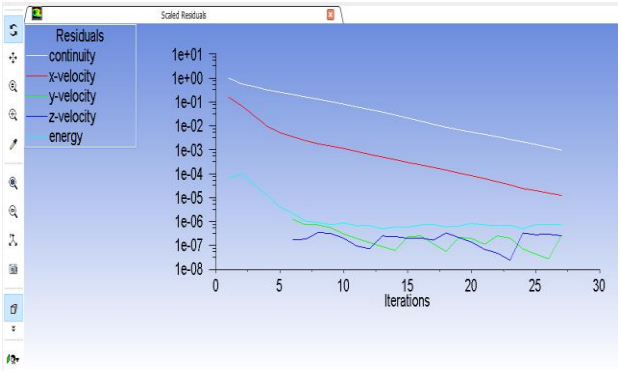

(a)

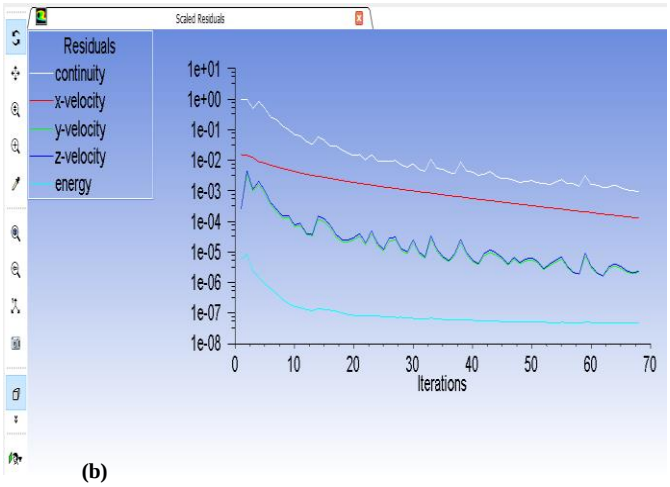

(b)

Figure 3: Scale residuals for the micro heat sink with (a) square and (b) circular configuration

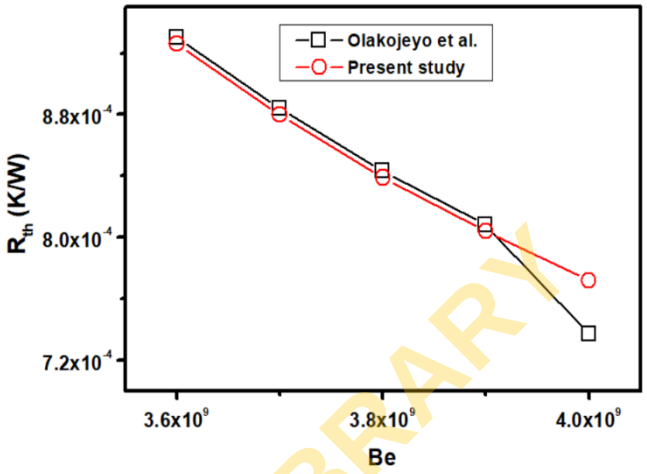

Figure 4: Code validation for thermal resistance against Bejan number

2) Grid refinement test and code validation of CFD

The mesh refinement was done until the size causing negligible changes in temperature was achieved. The line-by-line iteratively descretised solved equation was considered to have converged with the following convergence criterion:

$$\gamma = \left|\frac{(\Delta T_{max})_i - (\Delta T_{max})_{i-1}}{(\Delta T_{max})_i}\right| \leq 0.01 \quad (21)$$

where i is the number of iterations and $i-1$ gives the convergence condition once Eqn. (21) is satisfied.

The dimension of the unit cell computational domain used in this study is presented in Table 1. The computational domain was descretised using the hexahedral cell mesh setting. The mesh cells are increased continuously until stable mesh cells and nodes, corresponding to the stable maximum outlet wall temperature of less than 1% was obtained. Further refinement of the grid shows no significant difference in the outlet wall temperature. Therefore, to ensure accuracy, reduce computational time and cost, the mesh with nodes and cells 205 561 and 166 176, respectively are used for circular channel, and 117 338 and 144 440 for square cooling channels in the computation. Any increase in the nodes and cells, had no significant change on the numerical results.

Table 1: Dimensions of the microchannel heat sink used for grid refinement test

N (mm)	M (mm)	H (mm)	d_h (mm)	t_3 (mm)	$H-(t_1+d)$ (mm)
10	0.1	0.150	0.036	0.064	0.0687

Figure 4 shows calculations and comparisons of the global thermal resistance in the study of Olakoyejo *et al*. (2012) with the predicted results in this research within the Bejan number range $3.6 \times 10^9 \leq Be \leq 4.0 \times 10^9$. The results show that the values are in good agreement and the deviation between them is approximately 0.97% in thermal resistance. This disparity could be attributed to the difference in choice of d_s = 44.7 µm and t_3 = 55.3 µm used in Olakoyejo *et al*. (2012). However, the results of the correlation give assurances about the numerical process and code used in this present work.

IV. RESULTS AND DISCUSSION

The numerical simulation and optimisation are performed on the micro heat sink of varying total volume V of 0.15 to 0.17 mm^3 and fixed axial length of $N = 10\ mm$. The design space for the response surface is$36.3 \leq d_h \leq 46.7\ \mu m$, $t_1 \geq 50\ \mu m$,$56.3 \leq t_2 \leq 68.7\ \mu m$,$63.7 \leq t_3 \leq 66.6\ \mu m$, the width M is in the range 100 to 115 µm and the height H is in the range $148 \leq H \leq 150\ \mu m$. The range of porosity is $0.0691 \leq \phi \leq 0.0889$ for both square and circular cooling channels. The optimised design points are expected to meet the manufacturing restrictions. The objective function is to maximise the dimensionless global thermal conductance in the microchannel. The range of Reynolds number of the cooling fluid (water) through the microchannel of the heat sink is between Re_w =400 to 500. The thermal conductivity of the aluminium substrate used is 202.4 W/m K and the inlet temperature of water is 298 K.

The influence of dimensionless diameter on T_max is presented in Figure 5. At $Re_w = 500$, the value of dimensionless diameter increases in the range $0.0036 \leq \frac{d_h}{N} \leq 0.0041$, while T_max decreases. The curves show the existence of an optimal design variables that minimises the peak temperature at any point within the microchannel volume, which lies in the range $0.0036 \leq \frac{d_h}{N} \leq 0.0047$. The peak temperature decreases until the temperature corresponding to the optimised value is attained, any increase in the peak temperature beyond the optimised temperature increases in T_max, as seen in Figure 5. The trend in the figure (Figure 4) shows that the micro heat sink with square cooling channel performed better than the circular flow channel at T_{max} = 326.74 K and 348.74 K respectively, with $\frac{d_h}{N}$ lying between 0.0041 and 0.0042 for both configurations. The results show that the square cooling channels are preferred than the circular channels under the Reynolds number evaluated.

Figure 6 shows T_{max} as a function of optimised dimensionless diameter. The figure reveals the existence of an optimal dimensionless diameter that minimises the peak

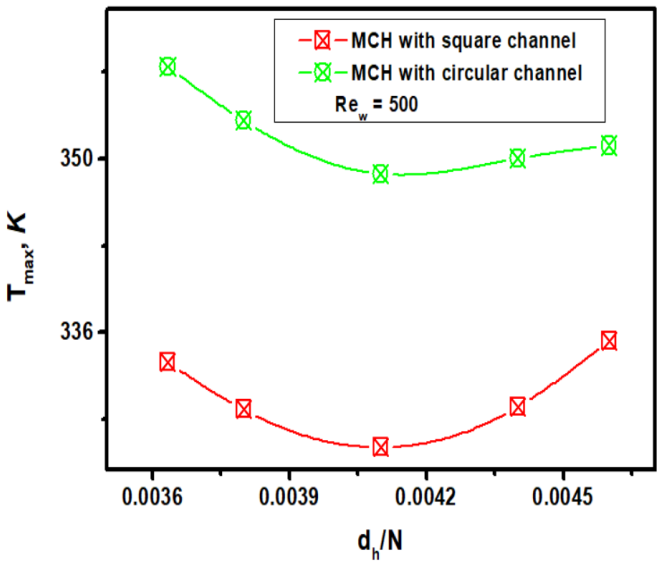

Figure 5: Influence of dimensionless diameter on peak temperature

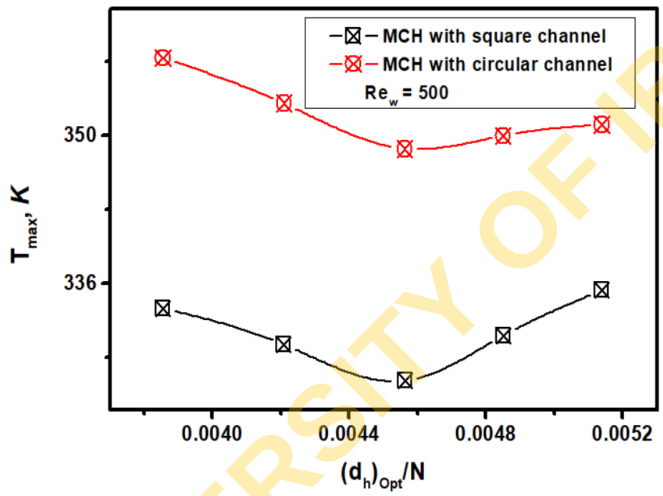

Figure 6: Influence of optimised dimensionless diameter on peak temperature

temperature in the cooling channel and in the entire volume of the microchannels with square and circular channels.

As $\frac{(d_h)_{Opt}}{N}$ increases, T_{max} decreases for $Re_w = 500$, as expected. The optimised value that corresponds to the minimised peak temperature lies in the vicinity of 0.0046. The trend in the results shows that the heat sink optimises at 326.74 and 348.74 K; any further increase in the dimensionless values increases the peak temperature.

The peak temperature for microchannel with circular channel increases gradually after the optimised temperature is reached, while in the micro heat sink with square channel increased sharply. The influence of Reynolds number on $(T_{max})_{min}$ is illustrated in Figure 7. The maximum minimum temperature decreases with increase in the fluid velocity. As the velocity of the fluid increases from 400 to 500, the minimised peak temperature $(T_{max})_{min}$ decreases by 2.2% in micro heat sink with square configurations and by 4.4% in micro heat sink with circular cooling channel.

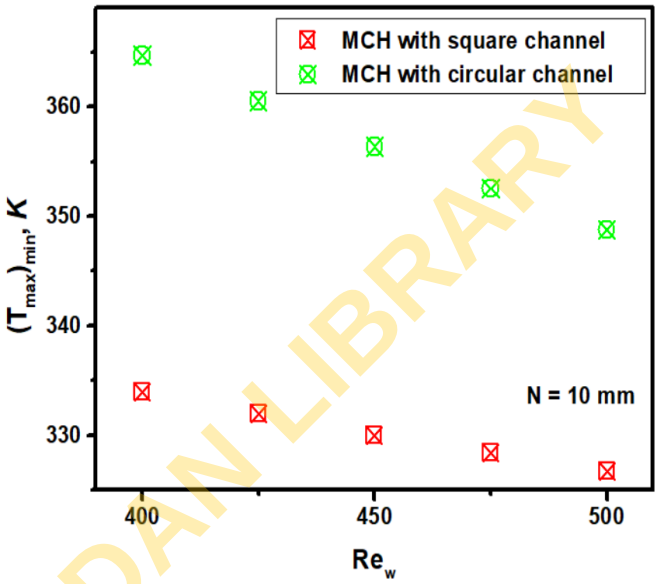

Fig. 7: Influence of Reynolds number on minimised temperature

Figure 8 shows that the C_{max} increases with increase in the Reynolds number, as expected. The global thermal conductance is enhanced by maximising global fluid flow access within the internal structure of the microchannel system based on constructal theory (Bejan & Lorente, 2004, 2011). The value of C_{max} increases by 20.1% in the square channels as compared by the circular flow channels with 23.9% increase in global thermal conductance.

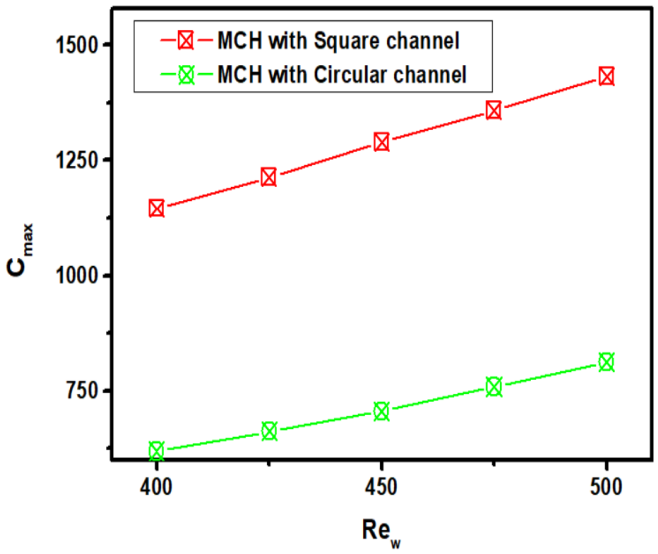

Figure 8: Influence of Reynolds number on global thermal conductance

Table 2 shows the summary of optimal design variables that corresponds to the minimised temperature in the outlet wall of a microchannel heat sink. The results are evaluated at a Reynolds number of 500 for the two configurations under

consideration. The summary of the optimisation results shows that the micro heat sink with square configuration has a minimised temperature of 326.74 K for an optimised hydraulic diameter of 0.0455 mm, corresponding to the optimised void fraction of 0.079 and external aspect ratio of 1.4.

Table 2: Summary of optimal values for $Re_w = 500$

Microchannel	Optimised hydraulic diameter $(d_h)_{Opt}$	Minimised temperature K	Optimised volume fraction $\left(\frac{V_s}{V}\right)_{Opt}$	Optimised external aspect ratio $\left(\frac{H}{M}\right)_{Opt}$
Square cooling channel	0.0455	326.74	0.0790	1.40
Circular cooling channel	0.0456	348.74	0.0790	1.40

In the case of the microchannel with circular flow channel, the minimised temperature is 348.74 K at an optimised hydraulic diameter of 0.0456 mm, optimised volume fraction of 0.079 and optimised $\left(\frac{H}{M}\right)_{Opt}$ of 1.4. The results reveal that the square configuration performed better than the circular cooling channels. This outcome agrees with previous research and authenticates the superiority of the square channels over the circular channels in traditional microchannel heat sinks.

V. CONCLUSION

In this paper, 3D-numerical optimisation of microchannel heat sink with square and circular configurations are presented. Micro heat sinks with fixed axial length and volume are simulated with high-density heat flux applied at the bottom surface. Single-phase water of Reynolds number between 400 to 500 was applied across the axial length of the microchannel to remove heat deposited at the bottom of the micro heat sink. The result of the optimisation reveals:

1) That the micro heat sinks perfomed well with the square configuration cools better than the circular channels.
2) That optimal hydraulic diameter parameters exists for both square and circular configurations in the range 34.36≤d_h≤41.76 μm, which sufficiently minimised peak temperature in the internal channel wall and in the entire volume of the micro heat sink.
3) That large quantity of heat flux can be removed and system cooled by increasing the velocity of the fluid pumped acrosss the micro heat sink.
4) That a highly-condcutive aluminium substrate is suitable for cooling microchannel heat sinks with fixed high-density heat flux.
5) That constructal technique approach used in evaluating the performance of the geometry for effective heat transfer is a viable method for enhancing thermal conductance.
6) That though the square design is better, the circular channels are prefered for industrial application and ease of manufacturing.
7) Finally, the two configurations investigated are judged good for cooling microelectronic packages and integrated circuitry.

ACKNOWLEDGMENT

The authors appreciate the support of Modibbo Adama University Yola and the University of Cape Town for the facilities used in carrying out this work.

AUTHOR CONTRIBUTIONS

N.Y. Godi: Conceptualization, Software, Validation, Writing -original draft, Methodology, **N.Y. Godi, L. B. Zhengwuvi, M. O. Petinrin:** Writing & editing, Validation.

REFERENCES

Bejan, A. (2000). Shape and structure, from engineering to nature. Cambridge University Press, UK.

Bejan, A. (2007). Why university rankings do not change: education as a natural hierarchical flow architecture. International Journal of Design & Nature and Ecodynamics, 2 (4): 319–327.

Bejan, A. (2009). Two hierarchies in science: The free flow of ideas and the academy. International Journal of Design and Nature and Ecodynamics, 4 (4): 386–394.

Bejan, A.; E. C. Jones and E. C. Charles. (2010). The evolution of speed in athletics: Why the fastest runners are black and swimmers white. International Journal of Design and Nature and Ecodynamics, 5 (3): 199–211.

Bejan, A. and Lorente, S. (2004). The constructal law and the thermodynamics of flow systems with configuration. International Journal of Heat and Mass Transfer, 47 (14–16): 3203–3214.

Bejan, A. and Lorente, S. (2006a). Design with Constructal Theory. International Journal of Engineering Education, 22 (1): 140–147.

Bejan, A. and Lorente, S. (2006b). Constructal theory of generation of configuration in nature and engineering. In Journal of Applied Physics, 100 (4).

Bejan, A. and Lorente, S. (2011). The constructal law and the evolution of design in nature. In Physics of Life Reviews, 8 (3): 209–240).

Bejan, A. and Marden, J. H. (2006). Unifying constructal theory for scale effects in running, swimming and flying. Journal of Experimental Biology, 209 (2): 238–248.

Bejan, A. and Sciubba, E. (1992). The optimal spacing of parallel plates cooled by forced convection. International Journal of Heat and Mass Transfer, 35 (12): 3259–3264.

Bello-Ochende, T.; L. Liebenberg and J. P. Meyer. (2007). Constructal cooling channels for micro-channel heat

sinks. International Journal of Heat and Mass Transfer, 50 (21–22): 4141–4150.

Chai, L.; G. Xia; M. Zhou and J. Li. (2011). Numerical simulation of fluid flow and heat transfer in a microchannel heat sink with offset fan-shaped reentrant cavities in sidewall. International Communications in Heat and Mass Transfer, 38 (5): 577–584.

Charles, J. D. and Bejan, A. (2009). The evolution of speed, size and shape in modern athletics. Journal of Experimental Biology, 212 (15): 2419–2425.

Chen, C. L. and Cheng, C. H. (2009). Numerical study of the effects of lid oscillation on the periodic flow pattern and convection heat transfer in a triangular cavity. International Communications in Heat and Mass Transfer, 36 (6): 590–596.

Chen, C.; S. Yang and M. Pan (2021). Microchannel structure optimization and experimental verification of a plate heat exchanger. International Journal of Heat and Mass Transfer, 175: 121385.

Gawali, B. S. and Kamble, D. A. (2011). Analysis of Rectangular Microchannel under Forced convection Heat Transfer condition. International Journal of Engineering Science and Technology, 3 (3): 2041–2043.

Gupta, D.; P. Saha and S. Roy. (2021). Computational analysis of perforation effect on the thermo-hydraulic performance of micro pin-fin heat sink. International Journal of Thermal Sciences, 163, 106857.

Hajialibabaei, M. and Saghir, M. Z. (2022). A critical review of the straight and wavy microchannel heat sink and the application in lithium-ion battery thermal management. International Journal of Thermofluids, 14: 100153.

Han, Y.; Y. Liu; M. Li and J. Huang. (2012). A review of development of micro-channel heat exchanger applied in air-conditioning system. Energy Procedia, 14: 148–153.

He, Z.; Y. Yan and Z. Zhang. (2021). Thermal management and temperature uniformity enhancement of electronic devices by micro heat sinks: A review. Energy, 216: 119223.

Ighalo, F. U. (2010). Optimisation of microchannels and micro pin-fin heat sinks with computational fluid dynamics in combination with a mathematical optimisation algorithm. Unpublished MSc. Thesis, Mechanical and Aeronautical Engineering, University of Pretoria, South Africa.

Ismail, L. S.; C. Ranganayakulu and R. K. Shah. (2009). Numerical study of flow patterns of compact plate-fin heat exchangers and generation of design data for offset and wavy fins. International Journal of Heat and Mass Transfer, 52 (17–18): 3972–3983.

Kern, D. Q., and Kraus, A. D. (1972). Extended surface heat transfer. McGraw-Hill.

Khan, M. N.;M. N. Karimi and M. O. Qidwai. (2022). Effect of circular perforated pin fin on heat transfer and fluid flow characteristics of rectangular microchannel heat sink. Numerical Heat Transfer, Part A: Applications, 1–15.

Khuri, A. I. and Mukhopadhyay, S. (2010). Response surface methodology. Wiley Interdisciplinary Reviews: Computational Statistics, 2 (2): 128–149.

Kose, H. A.; A. Yildizeli and S. Cadirci. (2022). Parametric study and optimization of microchannel heat sinks with various shapes. Applied Thermal Engineering, 211: 118368.

Laermer, F. and Urban, A. (2003). Challenges, developments and applications of silicon deep reactive ion etching. Microelectronic Engineering, 67–68: 349–355.

Lawal, A. Q.; O. O. Adewumi and O. T. Olakoyejo. (2022). Numerical Investigation of Thermal Performance of A Combined Heat Sink With Various Microchannel Shapes. Nigerian Journal of Technological Development, 19 (2): 164–171.

Le, H. S.; A. M. Galal; I. Alhamrouni; A. A. Aly; M. Abbas; A. S. Saidi; T. H.Truong; M. Dahari and Wae-hayee, M. (2022). Heat transfer efficiency optimization of a multi-nozzle micro-channel heat sink utilizing response surface methodology. Case Studies in Thermal Engineering, 37: 102266.

Li, W.; Z. Xie; K. Xi; S. Xia and Y. Ge. (2021). Constructal optimization of rectangular microchannel heat sink with porous medium for entropy generation minimization. Entropy, 23 (11).

Li, Y.; F. Zhang; B. Sunden and G. Xie. (2014). Laminar thermal performance of microchannel heat sinks with constructal vertical Y-shaped bifurcation plates. Applied Thermal Engineering, 73 (1): 185–195.

Madou, M. J. (2018). Fundamentals of Microfabrication, CRC Press, Boca Raton, USA.

Myers, R. H.; D. C. Montgomery and C. M. Anderson-Cook. (2016). Response Surface Methodology: Process and Product Optimization Using Designed Experiments (4th ed.). John Wiley & Sons, Hoboken.

Olakoyejo, O. T.; T. Bello-Ochende and J. P. Meyer (2012). Mathematical optimisation of laminar forced convection heat transfer through a vascularised solid with square channels. International Journal of Heat and Mass Transfer, 55 (9–10): 2402–2411.

Patel, V. U., and Modi, A. J. (2012). Optimization of heat sink analysis for electronics cooling. World Journal of Science and Technology, 2 (4): 64–69.

Qiu, J.; J. Zhou; Q. Zhao; H. Qin and X. Chen. (2021). Numerical investigation of flow boiling characteristics in cobweb-shaped microchannel heat sink. Case Studies in Thermal Engineering, 28: 101677.

Reis, A. H.; A. F. Miguel and M. Aydin (2004). Constructal theory of flow architecture of the lungs. Medical Physics, 31 (5): 1135–1140.

Sun, K.; H. Feng; L. Chen and Y. Ge. (2022). Constructal design of a cooling channel with semi-circular sidewall ribs in a rectangular heat generation body. International Communications in Heat and Mass Transfer, 134: 106040.

Weinerth, G. (2010). The constructal analysis of warfare. International Journal of Design and Nature and Ecodynamics, 5 (3): 268–276.

Xie, G.; F. Zhang; B. Sundén and W. Zhang. (2014). Constructal design and thermal analysis of microchannel heat sinks with multistage bifurcations in single-phase liquid flow. Applied Thermal Engineering, 62 (2): 791–802.